Review article

Microracks Detection Techniques in Silicon Solar Cell

.

ABSTRACT

Due to very high demand and increasing price of fossil fuels, major research is going on in the area of renewable energy especially solar energy. Cost of solar cell which is major source to convert solar energy into electrical energy dependents on the raw silicon which is very expensive. Therefore, to overcome the effect of cost of solar cell, it is necessary to check the silicon wafer before inline processing in making of solar cells and solar panels. In this article we presented various efforts by various researchers to find out micro cracks in the solar cell and solar wafers. This article gives various methods and their comparative study for finding crack in solar cells.

Keywords: LBIC, EBIC, Micro-crack, Solar Cell, Solar wafer

1. INTRODUCTION

Due to the high cost and limited stock of energy sources available on the earth, renewable energy sources got high attention for research. In contrast, the many types of renewable energy resources such as wind and solar energy-are constantly replenished and will never run out. Solar energy is the photonic energy which is converted into electrical energy by solar cell. Solar cell can be categorized into inorganic solar cell and organic solar cell. In this study we are focusing on the inorganic silicon solar cell. It is important to recognize that the silicon wafer is a large contributor, up to 75%, to the overall cost of the solar cell [1] and the silicon raw material price increased exponentially due to a worldwide shortage of polycrystalline silicon. To compensate for the feedstock shortage of silicon, solar wafer manufacturers are slicing silicon thinner and thinner with thicknesses down to order of 100µm or lesser [2]. Figure 1 shows typical flow in the production of wafers from silicon. Wire saw technology is being used by [2]; it is the technology for slicing thin wafer from a large diameter crystalline ingot of silicon. Wire saw must be balance precisely to achieve higher productivity while minimizing the breakage problem in the wafer. In addition to the reduction of the thickness, wafer's manufacturers are also increasing the size of the wafer in order to reduce the overall production cost. Solar wafers of size up to 210 mm × 210 mm square shaped are now available in the current market.

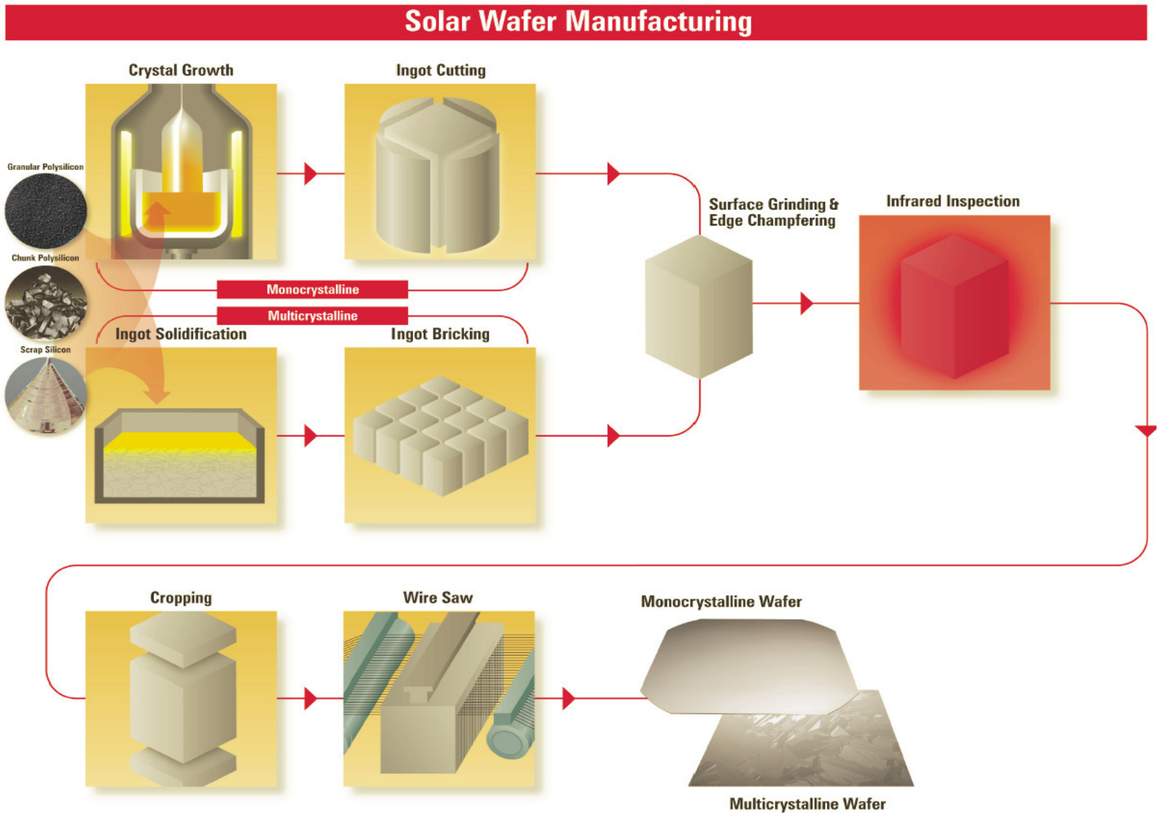

Fig. 1. Typical process flow in the production of crystalline silicon wafers [2]

These technological trends in the production make wafer handling more challenging as the processes can potentially reduce the yield due to increased wafer and cell breakage. Typically, the handling or mishandling may lead to some physical defects in the wafer like cracks or scratches. These cracks may vary from macro level to micro level, generally, the cracks of width of order less than 100 µm are considered as micro-cracks. Both polycrystalline and mono crystalline solar wafer/cell occasionally contains micro-cracks. Figure 2 illustrates example of the polycrystalline solar wafer with micro-crack. This figure 2 shows micro-crack which has been indicated by an arrow symbol. Low gray level and high gradient magnitudes are two main features for the micro-cracks in solar wafers. Due to its size, naturally this type of defect cannot be seen by naked eyes. Consequently, this may result in the production of inferior quality solar panels if this defect in solar wafers or cells goes undetected. In worst case the cell might even fail and this leads to the potentially malfunctioned photovoltaic (PV) modules [3]. Also, it can be seen from the figure 2, the picture of the polycrystalline solar wafer shows multiple grains of different shapes and sizes, therefore it is very hard to differentiate between micro-crack and grain boundary by simple machine vision learning. So it is important to develop an inspection system for the detection and evaluation of such a defect. Preferably, such a system should be non-contact in order to ensure the surface and subsurface integrity of silicon wafers is preserved before and after assessment, and from the start of the production process till completion [4]. The main objective of this paper is to review some of the well-known and emerging technologies for micro-crack detection of solar wafers. Some of the salient features of these methods are identified and critically discussed; aiming to provide useful guidance to new and existing researchers wishing to venture into this very interesting research area.

Fig. 2. Example of polycrystalline solar wafer with micro-crack

2. MICRO-CRACK INSPECTION IN SOLAR WAFERS/CELLS

To-date various researchers have experimented various methods and techniques for the detection of micro-crack in solar wafers and solar cells. The most common methods that have been investigated include the laser beam induced current (LBIC) [5-8], the electron beam induced current (EBIC) [9-11], the optical testing such as the photoluminescence [12-14] the electroluminescence imaging [15]. In this paper, all the aforementioned methods will be reviewed, highlighting some of their salient characteristics including merits and demerits. For completion and thoroughness, some image processing techniques for the shape and size detection of micro-cracks will also be discussed.

2.1 Laser Beam Induced Current (LBIC)

LBIC is a non-destructive optical testing for the characterization of semiconductors [16-17]. The basic LBIC system setup is shown in figure 3. As shown in this figure, the light source is selected from laser diodes of different wavelengths between 638 and 850 nm, and an electrical current to the laser diode is electronically modulated to produce an AC laser beam, and the modulation also provides the reference signal for a lock-in amplifier. When a light beam is scanned over the surface of a photosensitive device, it creates electron-hole pairs in the semiconductor causing a the dc current to flow which in turn measured using suitable devices [5-8]. Such measurements are repeated for different position of the laser beam to obtain LBIC image of the sample. The variations in the current are recorded and converted into variation in contrast forming the LBIC image. More variation in the current indicates that the cell will be more defected. In a typical set-up, the LBIC technique consists of a calibrated measurement of current and reflection coefficient. This information allows the internal quantum efficiency (IQE) of the solar cell is assessed [18]. The IQE is defined as the fraction of incident photons transmitted into the solar cell that contribute in the generation of electron-hole pairs. Mathematically it is given by [19]:

$$IQE = \frac{1}{1-R}\left[\frac{h\ c\ I_{sc}}{e\ \lambda\ I_L}\right] \quad (1)$$

where R is reflection coefficient, h is Planck's constant, c is velocity of light, e is electron charge, λ is wavelength of the illuminating light, I_{SC} is measured short circuit current and I_L is intensity of the illuminated light. The quantum efficiency is the photon to electron conversion efficiency of the solar cell. Hence, lesser the efficiency of the cell indicates that the cell is more defective.

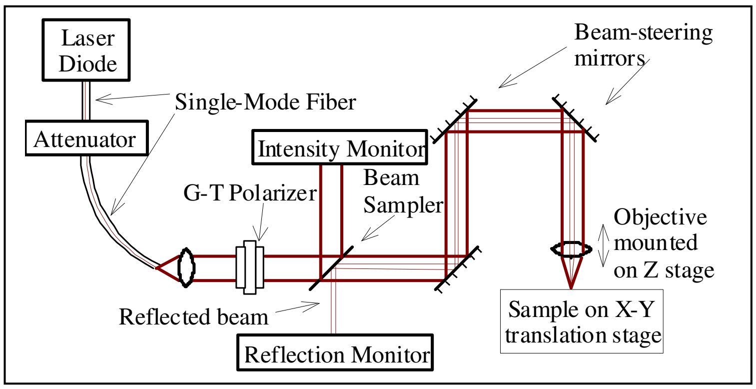

Fig. 3. LBIC Measurement Setup

Figure 4 shows the current distribution map of the cell obtained through LBIC imaging. In this figure, the dark irregular lines correspond to the active performance degrading grain boundaries. Figure 5(a) shows the LBIC reflection map corresponding to the darker areas of Figure 4. It is evident that the current distribution, as expected for multi-crystalline material, is not uniform as illustrated in regions marked A–C. The uniformity is compromised by the reflection and absorption of different grains at the surface of the polycrystalline silicon solar cell. Light is reflected more in region C than the neighboring regions A and B. In Figure 5(b), reflective line scan is depicted, which further indicates the high current response in region C. This region is expected to decrease the efficiency of the solar cell when it is in operation. The feature indicated by X corresponds to the grain boundary which clearly reflects more incident light as do the contact fingers.

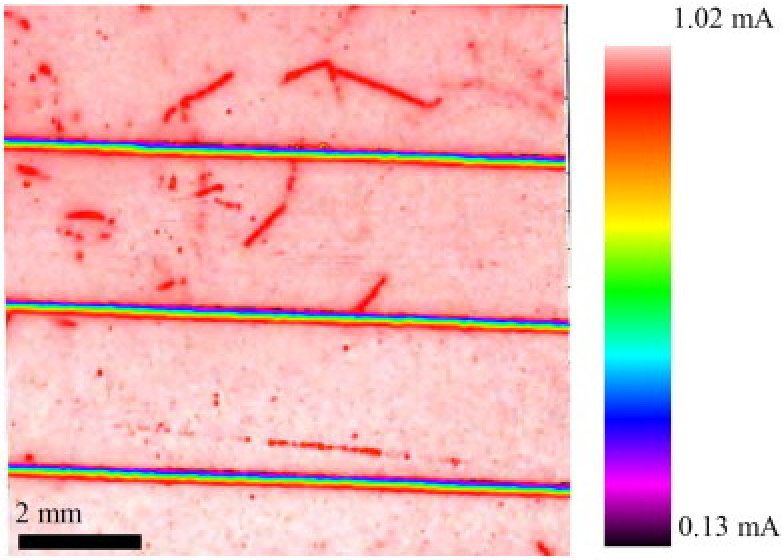

Fig. 4. LBIC map of Polycrystalline silicon solar cell [18]

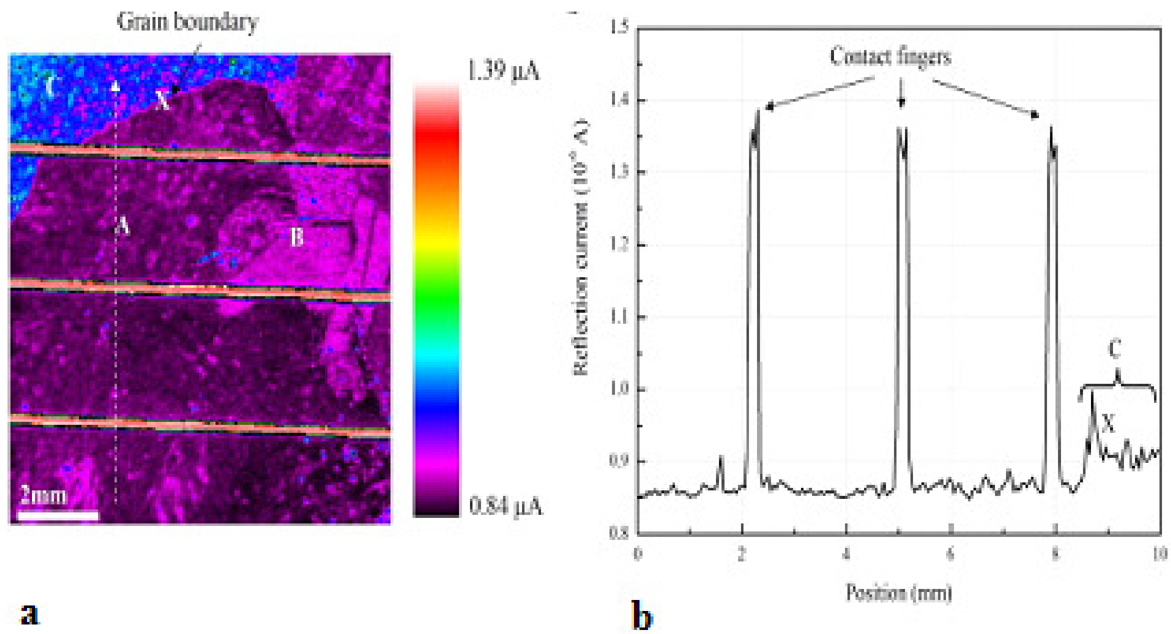

Fig. 5. (a) Reflection map and (b) reflection current map corresponding to image in figure 4 [18]

Laser beam induced current (LBIC) methods have been investigated both for fast line scan techniques and for detailed surface mapping [20]. The major drawback of this method lies in the necessity for electrical contacts, making this technique nearly impossible to apply for wafer inspection and technically difficult for non-tabbed solar cells. Furthermore, the scanning needs to be performed for the entire wafer area and this process is prohibitedly time consuming even though the accuracy of the LBIC is acceptable.

2.2 Electron Beam Induced Current (EBIC)

EBIC analysis, as the name implies, is a semiconductor analysis technique that employs an electron beam to induce a current within a sample which may be used as a signal for generating images that depict characteristics of the sample, among others showing the locations of p-n junctions in the sample, highlighting the presence of local defects, and mapping doping non-homogeneities [21]. Since a scanning electron microscope (SEM) is a convenient source of electron beam for this purpose, most EBIC techniques are performed using a SEM. A typical EBIC imaging system consisting, SEM, low noise current amplifier and display unit is shown in figure 6. When an electron beam from SEM strikes the surface of the solar cell, it generates the electron-hole pairs within the volume of beam interaction over the cell.

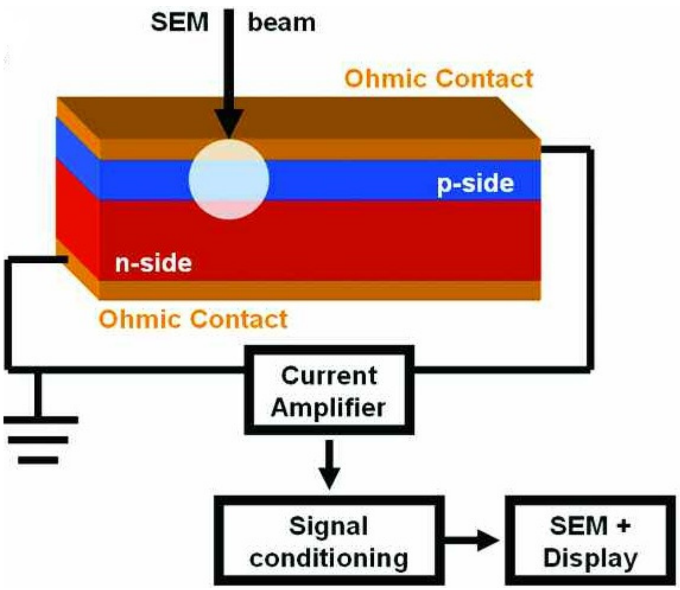

Fig. 6. EBIC Imaging Systems

With proper electrical contact with the sample, the movement of the holes and electrons generated by the SEM's electron beam can be collected, amplified, and analysed, such that variations in the generation, drift, or recombination of these carriers can be displayed as variations of contrast as in LBIC image discussed previously. EBIC imaging is very sensitive to electron-hole recombination. This is the reason, why EBIC analysis is very useful for finding defects that act as recombination centres in semiconductor materials. The EBIC current (I_{EBIC}) collected is many times larger than the primary beam current absorbed by the sample (I_{ab}), and is given by the equation

$$I_{EBIC} = I_{ab} \times \left(\frac{E_b}{E_h} \right) \times n \qquad (2)$$

where E_b is the primary beam energy or the SEM's accelerating voltage, E_h is the energy needed to create an electron-hole pair (about 3.6 eV for Silicon), and n is the collection efficiency. The accelerating voltage belongs to the extremely high Tension (EHT) category, ranging from tens to hundreds of keV. Thus, assuming a collection efficiency of 100%, and an EHT of 20 keV, the collected EBIC current would be about 5556 times larger than I_{ab}. EBIC currents are usually in the nanoampere to microampere range while I_{ab} is in the picoampere range. In areas around the p-n junction where physical defects exist, electron-hole recombination is enhanced, thus reducing the collected current in those defected areas. Hence, if the current through the junction is used to produce the EBIC image, the areas with physical defects will appear to be darker in the EBIC image than areas with no physical defects. EBIC imaging is therefore a convenient tool for finding sub-surface and other difficult-to-see damage sites.

Referring to figure 6, the wire that carries the current away from the top contact can be seen in the lower left. The solar cell is slowly scanned and the EBIC current given by Equation (2) is then measured. This current is displayed in colour. The measured EBIC current was small when the beam fell on the metal contact but was larger when it fell on the active region of the solar cell. Figure 7 shows a secondary electron image of a polycrystalline silicon solar cell. Within the active region of the solar cell there are large variations in the current. This is due to a variation in the density of defects which causes the electron-hole pairs to recombine before they are separated by the built-in electric field. Figure 8 illustrates a typical EBIC image when the electron beam energy is 20 keV [11]. The crack can be clearly seen in the image. Therefore this technique is useful to detect the presence or absence of micro-crack in solar cell or solar wafer.

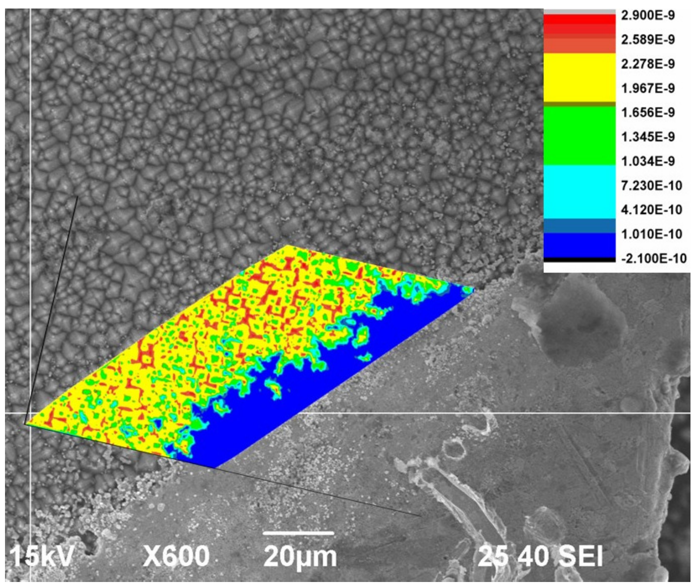

Fig. 7. EBIC current map of a polycrystalline silicon solar cell

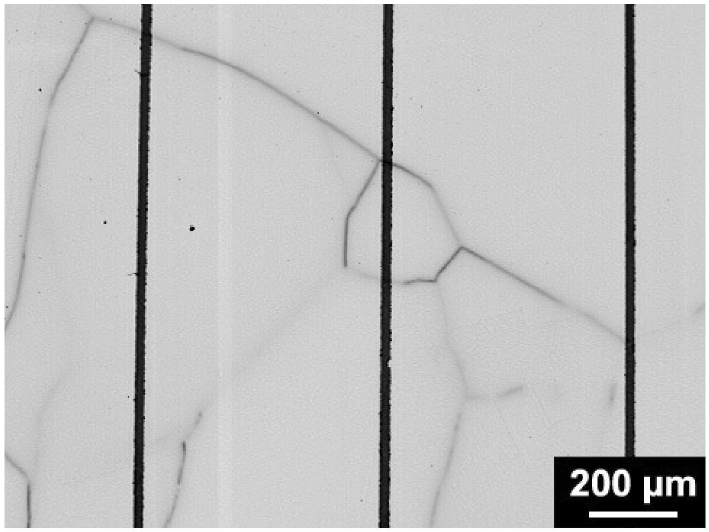

Fig. 8 Example of EBIC image captured at 20 keV excitation [11]

EBIC and LBIC are powerful tools for mapping distribution of recombination active defects and impurities in solar cells. The operation of both EBIC and LBIC is based on local injection of minority carriers and their subsequent collection by a p-n junction or a Schottky diode fabricated on the sample surface, the measurement closely mimics the actual operation of a solar cell. LBIC, which has somewhat lower resolution than EBIC, is usually used to map the whole cell, whereas EBIC is better suited for high resolution imaging of small areas of the wafer. The analysis of temperature dependence of EBIC contrast enables one to distinguish shallow and deep recombination centers, but no further parameters of the traps can be determined. Additionally, the depth of the analyzed layer is shallow, typically several microns from the surface in EBIC, and several tens or hundreds of microns in LBIC, depending on the wavelength of the illuminator. Therefore, only a small fraction of the sample volume in which electron–hole pairs are generated can be analyzed.

2.3 Electroluminescence (EL) imaging technique

Luminescence imaging is very attractive idea for the micro-crack detection for the solar cells and wafers. Luminescence in the semiconductor is the result of the electron-hole recombination by electron excitation. Electroluminescence (EL) is the form of luminescence in which electrons are excited into the conduction band through the use of electrical current by connecting cell in forward bias mode. This technique could be applied not only to the finished cell but also to the module and solar panels. The typical set-up for electroluminescence based inspection system is shown in Figure 9. It shows the solar cell sample connected to a power supply, a Silicon-CCD camera used to capture the picture which is then processed by the work station.

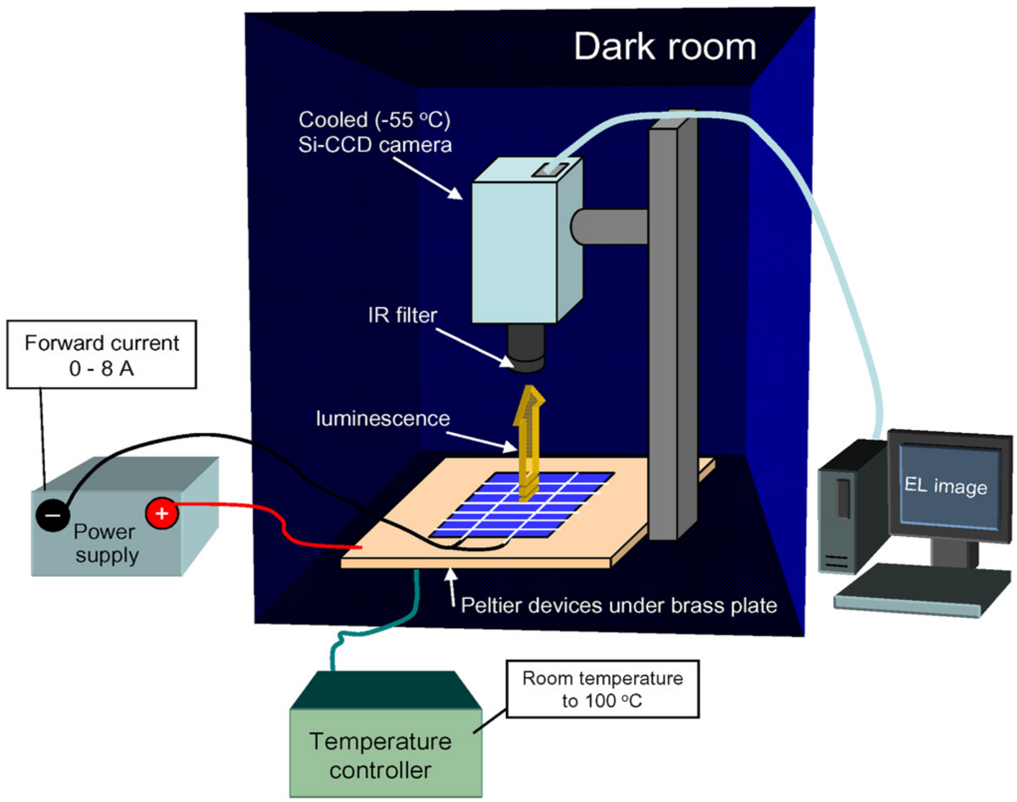

Fig. 9. A typical set up for Electroluminescence [15]

EL method requires the solar cells to be in the forward bias condition in order for it to emit infrared radiations. The luminescence ranges from 950 nm to 1250 nm with the peak occurring at approximately 1150 nm. Emission intensity is dependent on the density of defects in the silicon, with fewer defects resulting in more emitted photons. The EL system should be placed in the dark room as the image of the cells is being taken by cooled charge couple devices (CCD) camera.

Figure 10 (a) shows the sample of optical image of the defected monocrystalline silicon solar cell, whereas Figure 10(b) shows the EL image of the same cell. The presence of horizontal line can easily be seen in the bottom part of the Figure 10(b). This horizontal line is a crack present in the cell which cannot be seen in the Figure 10(a). Meanwhile Figure 10(d) shows an EL image of the polycrystalline silicon cell in which the grain boundaries became visible; those are not visible in the optical image as shown in Figure 10(c). The beauty of this system is that it can be applied for the wafer, cell as well as photovoltaic module. Figure 11 shows EL image of the monocrystalline photovoltaic (PV) module reported by [22]. The CCD image of the monocrystalline photovoltaic module acquired at delivery is shown in Figure 11(a), while Figure 11(b) shows the corresponding EL image. The presence of manufacturing defects like crack in the module is not clearly visible in Figure 11(a).

From the results given above, it is clear that the EL imaging is a good technique to inspect the defects in the solar cell. But this method also requires electrical contacts between the cell and the leads supplying currents from an external power supply. Therefore, this method works well for cells and modules, but not for wafers. However, with wafers the radiation can also be induced by illuminating it with source of a smaller wavelength: the so called photo-luminescence (PL). The details are explained in the following section.

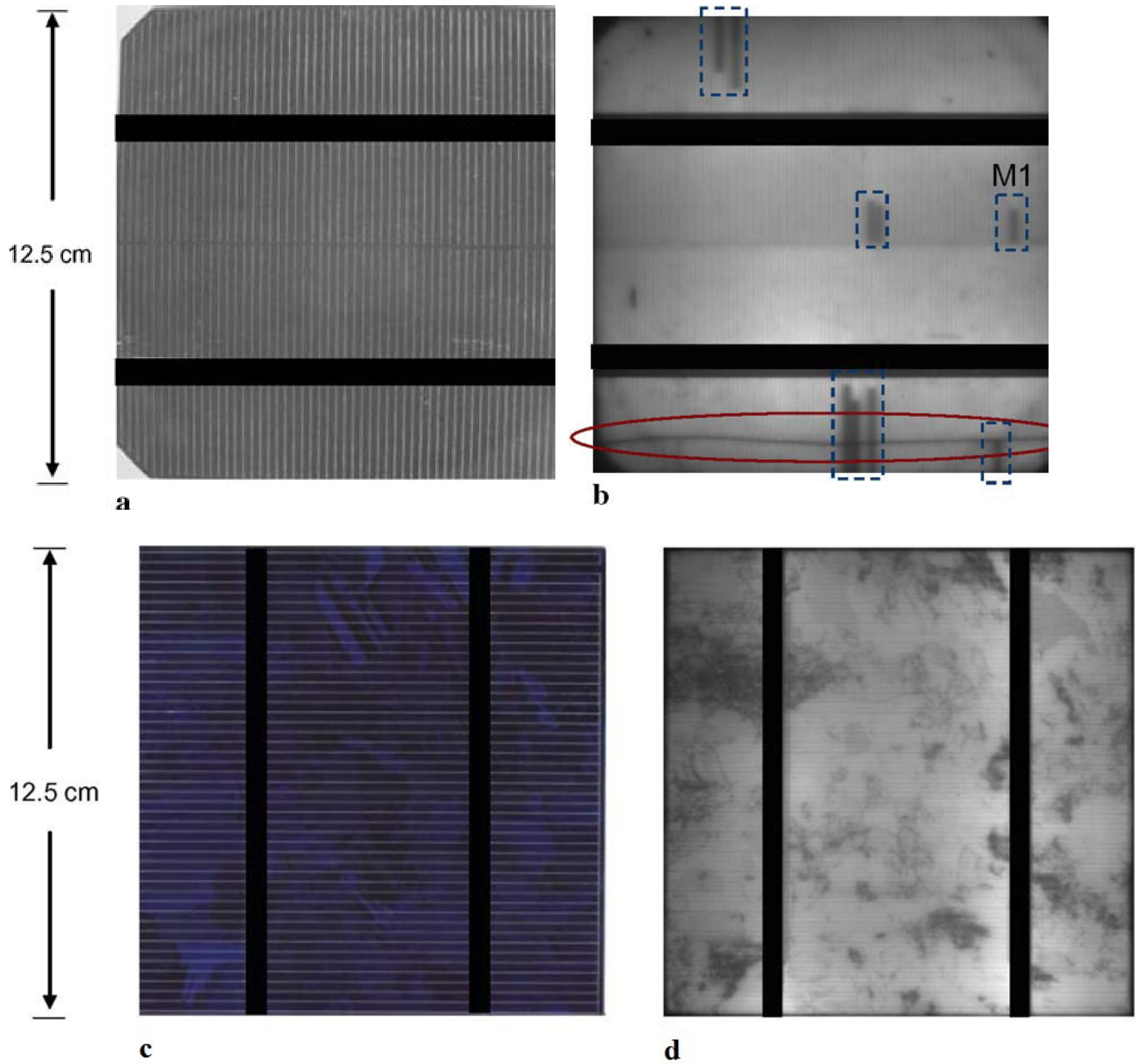

Fig. 10. (a) Optical image of a defected monocrystalline silicon solar cell, (b) the corresponding EL image of (a), (c) optical image of defected polycrystalline silicon solar cell, (d) the corresponding EL image of (c) [15]

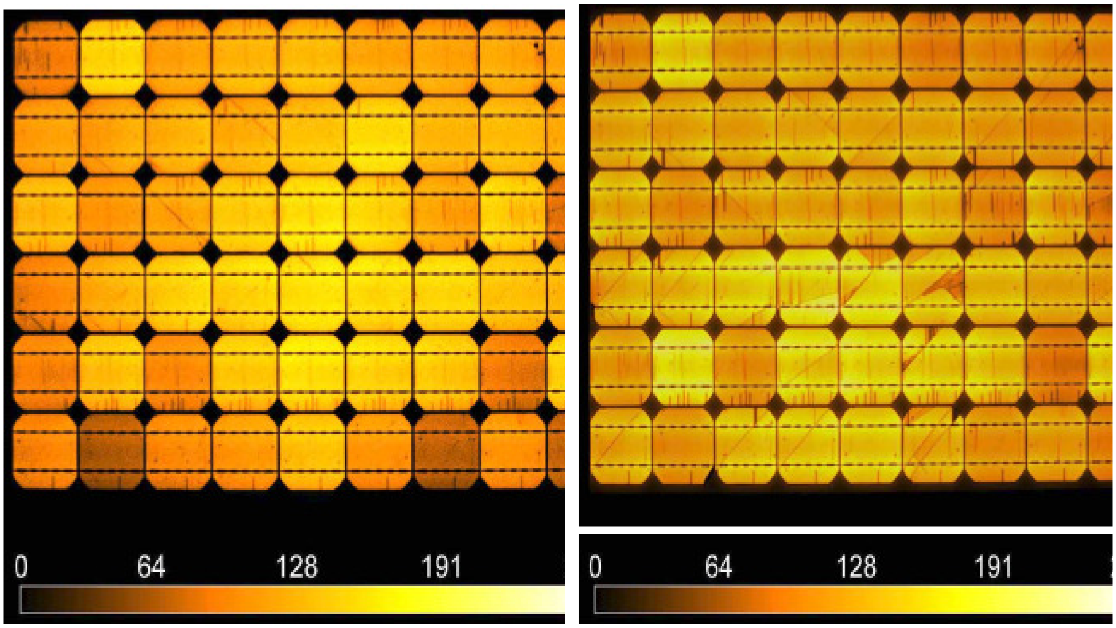

(a)

(b)

Fig. 11. EL images of a PV module (a) at delivery status (b) after exposed to temperature change

2.4 Photoluminescence (PL) imaging technique

As explained in previous section, the EL is very efficient technique to locate the defects in the solar cell but it can be applied for finished cell or module only. This method cannot be applied in the case of solar wafer. Photoluminescence (PL) is a versatile non-destructive tool to inspect silicon wafers and solar cells. More importantly, this method eradicates the needs for an electrical contact with the device under test. Moreover it can be applied not only at the end of the cells production, but it can be slotted in during the processes of producing solar cells [23].

Photoluminescence is the result of the electron-hole recombination in which the electron excited to the conduction band after absorption of photon. The imaging setup is very similar to the EL. The only difference is the electrons are excited by means of laser source as shown in figure 12 [12]. The PL image is detected using a cooled CCD camera with a 1000nm long pass filter to remove the reflected and scattered laser light.

Physics behind the PL imaging is that most of the photon generated electrons give up their energy as heat, but a small fraction of the electrons recombine with a hole, emitting a photon (radiative recombination). The photoluminescence intensity depends on the rate of recombination of electron-hole pairs, which depends on the excess carrier density and the doping concentration in the semiconductor. If we consider the case of p-type solar wafer with doping concentration N_A and Δn is the excess minority carrier density then the intensity of the PL current is given as follows [24]:

$$I_{PL} \,\alpha\, R \approx B\,\Delta n\,(\Delta n + N_A) \quad (3)$$

where *R* and *B* are radiative recombination rate and radiative recombination coefficient respectively. Photoluminescence intensity is proportional to the carrier concentration. Therefore, bright areas in general indicate higher minority-carrier lifetime regions, whereas dark areas indicate higher defect concentration.

More defects in the silicon will result in more energy lost as heat, and fewer emitted photons. In contrast fewer defects in the silicon will result in more radiative recombination, and more emitted photons. Example of the PL image of the polycrystalline silicon solar cell is given in figure 13 [25], showing the presence of micro-cracks and they are highlighted in a red square box. PL imaging is an efficient technique as it does not require any electrical contact and the image taken by this technique is free from series resistance. It can be applied to wafer, cell as well as module.

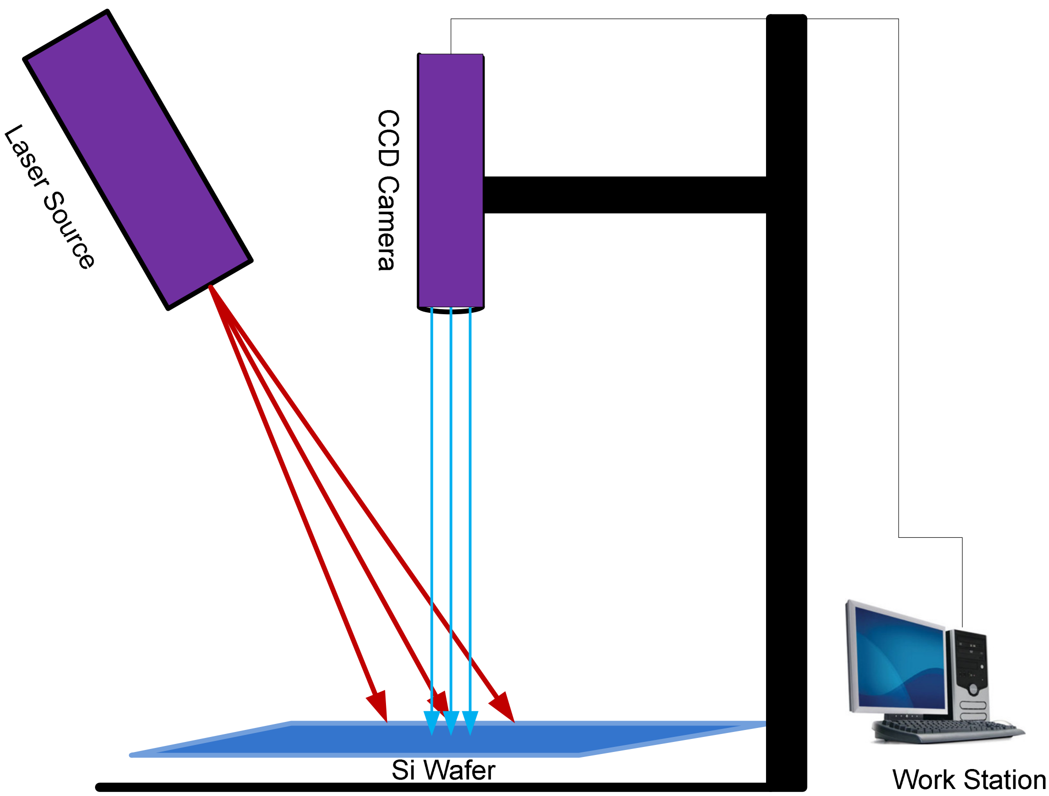

Fig. 12. Typical photoluminescence imaging setup

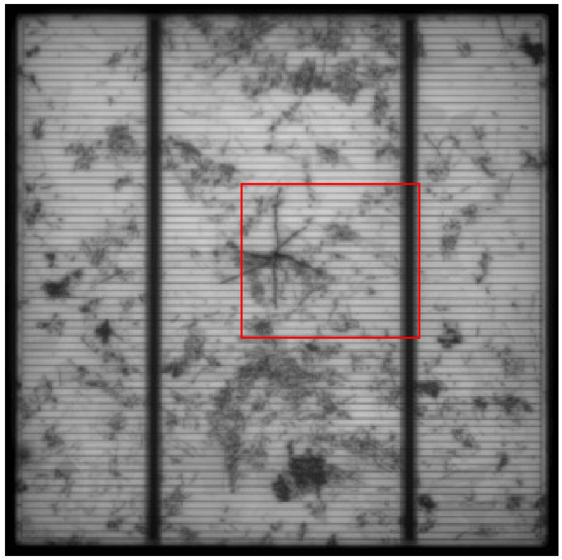

Fig. 13. Example of PL image of a polycrystalline silicon solar cell with micro-crack in the red box

3. CONCLUSION

In this paper the first laser beam induced current testing method is investigated, although it is very good technique for the in line testing but the major drawback of this method is that it needs electrical contacts with the cell. Second technique discussed here is based on electron-hole recombination which is the electron beam induced current. Like LBIC method EBIC method is also not applicable to the solar wafer because it also needs electrical contacts. EBIC analysis is very useful for finding defects that act as recombination centers in solar cells. Electroluminescence and photoluminescence is also discussed in this article gave high quality results. But between these EL and PL techniques PL is better than EL as it can be applied for solar wafers as well as solar cells.

REFERENCES:

1. **Zimmermann**, C.G. 2006: The impact of mechanical defects on the reliability of solar cells in aerospace applications. *IEEE Transactions on Device and Materials Reliability* 6, 486–494.
2. **MEMC**, June 2011, http://www.memc.com/index.php?view=Solar-Manufacturing.
3. **Kontges**, M., Kunze, I., Kajari-Schroder S., Breitenmoser, X. and Bjorneklett, B. 2011: The risk of power loss in crystalline silicon based photovoltaic modules due to micro-cracks. *Solar Energy Materials & Solar Cells* 95, 1131 – 1137.
4. **Dunlop**, E.D. and Halton, D. 2004: Radiometric pulse and thermal imaging methods for the detection of physical defects in solar cells and Si wafers in a production environment. *Solar Energy Materials and Solar Cells* 82, 467 – 480.
5. **Carstensen**, J, Popkirov, G., Bahr, J. and Foll, H. 2003: CELLO: an advanced LBIC measurement technique for solar cell local characterization. *Solar Energy Materials and Solar Cells 76*, 599-611.
6. **Sites**, J.R. and Nagle, T.J. 2005: LBIC analysis of thin-film polycrystalline solar cells. *Proceedings of* 31^{st} *PVSC Photovoltaic Specialists Conference.* Fort Collins, 199 – 204.
7. **Vorster**, F.J. and Dyk, E.E.V. 2007: High saturation solar light beam induced current scanning of solar cells. *Review of Scientific Instrument* 78, 013904-1-8.
8. **Zook**, J.D. 1980: Effects of grain boundaries in polycrystalline solar cells. *Applied Physics Letter 37*, 223-226.

9. **Breitenstein**, O., Bauer, J., Kittler, M., Arguirov, T. and Seifert W. 2008: EBIC and luminescence studies of defects in solar cells. *Scanning* 30, 331 – 338.

10. **Kittler**, M., Kveder, V.V. and Schroter, W. 1999: Temperature dependence of the recombination activity at contaminated dislocations in Si: A model describing the different EBIC contrasts behaviour. *Diffusion and Defect Data Pt. B.: Solid State Phenomena* 69, 417-422.

11. **Meng**, L., Nagalingam, D., Bhatia, C.S., Street, A.G. and Phang, J.C.H. 2010: SEAM and EBIC studies of morphological and electrical defects in polycrystalline silicon solar cell. *Proceedings of IEEE International Reliability Physics Symposium*. Singapore, 503-507.

12. Israil, Mohd, Said Amirul Anwar, and Mohd Zaid Abdullah. "Automatic detection of micro-crack in solar wafers and cells: a review." *Transactions of the Institute of Measurement and Control* (2012).

13. **Giesecke**, J.A., Michl, B., Schindler, F., Schubert, M.C. and Warta, W. 2011: Minority carrier lifetime of silicon solar cells from quasi-steady-state photoluminescence. *Solar Energy and Materials* 95, 1979-1982.

14. **Trupke**, T., Bardos, R.A., Schubert M.C. and Warta, W. 2006: Photoluminescence imaging of silicon wafers. *Applied Physics Letters* 89, 0441071-3.

15. **Fuyuki**, T. and Kitiyanan, A. 2009: Photographic diagnosis of crystalline silicon solar cells utilizing electroluminescence. *Applied Physics A: Materials Science & Processing* 96, 189–196.

16. **Bajaj**, J., Bubulac, L.O., Newman, P.R., Tennant, W.E. and Raccah, P.M. 1993: Spatial mapping of electrically active defects in HgCdTe using laser beam induced current by scanning laser microscopy. *Semiconductor Science and Technology* 5, 3186–3189.

17. **Bajaj**, J., and Tennant, W.E. 1990: Remote contact LBIC imaging of defects in semiconductors. *Journal of Crystal Growth* 103,170–178.

18. **Thantsha**, N.M., Macabebe, E.Q.B., Vorester, F.J. and Dyk, E.E.V. 2009: Opto-electronic analysis of silicon cell by LBIC investigations and current-voltage characterization. *Physica B* 404, 4445-4448.

19. **Mazer**, J.A. 1996: *Solar Cell: An Introduction to Crystalline Photovoltaic Technology.* Boston: Kluwer Academic.

20. **Agostinelli,** G., Friesen, G., Merli, F., Dunlop, E.D., Acciarri, M., Racz, A., Hylton, J., Einhaus, R. and Lauinger, T. 2001: Large area fast LBIC as a tool for inline PV module string characterisation, *Proceedings of the 17th European Photovoltaic Solar Energy Conference*. Munich, 410-413.

21. **Leamy**, H.J. 1982: Charge Collection Scanning Electron Microscopy. *Journal of Applied Physics* 53, R51-R80.

22. **Sander**, M., Henke, B., Schweizer, S., Ebert, M. and Bagdahn, J. 2010: PV module defect detection by combination of mechanical and electrical analysis methods. *Proceedings of 35th PVSC Photovoltaic Specialists Conference Photovoltaic Specialists Conference (PVSC)*. Hawaii, 1765-1769.

23. **Abbott**, M.D., Cotter, J.E., Trupke, T., Fisher, K. and Bardos, R.A. 2006: Application of Photoluminescence to High-Efficiency Silicon Solar Cell Fabrication. *Proceedings of the 4th World Conference on Photovoltaic Energy Conversion*. Waikoloa. Volume 1, 1211-1214.

24. **Herlufsen**, S., Schmidt, J., Hinken, D., Bothe, K. and Brendel, R. 2008: Photo conductance-calibrated photoluminescence lifetime imaging of crystalline silicon, Physica Status Solidi (RRL) 2, 245–247.

25. **Kingdom-tech (KT)**, http://www.kingdom-tech.com.cn/uploadfile/download/f/1/6_1306387325.pdf, last retrieved 3 Dec., 11.